Title
Temperature Dependence of Water Interactions with the Amide Carbonyls of α-Helices

Journal
Biochemistry, 51(26)

ISSN
0006-2960

Authors
Brewer, Scott H
Tang, Yuefeng
Vu, Dung M
et al.

Publication Date
2012-07-03

DOI
10.1021/bi3006434

Peer reviewed

Published in final edited form as:
Biochemistry. 2012 July 3; 51(26): 5293–5299. doi:10.1021/bi3006434.

Temperature Dependence of Water Interactions with the Amide Carbonyls of *α*-Helices

Scott H. Brewer[†], **Yuefeng Tang**[‖], **Dung M. Vu**[§], **S. Gnanakaran**[§], **Daniel P. Raleigh**[‖], and **R. Brian Dyer**[*,‡]

[†]Department of Chemistry, Franklin & Marshall College, Lancaster, Pennsylvania 17604-3003, United States

[§]Los Alamos National Laboratory, Chemistry Division, Group PCS, Mail Stop J567, Los Alamos, New Mexico 87545, United States

[‖]Department of Chemistry, State University of New York at Stony Brook, Stony Brook, New York 11794, United States

[‡]Department of Chemistry, Emory University, Atlanta, Georgia 30322, United States

Abstract

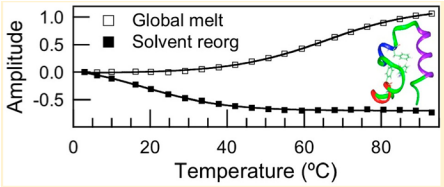

Hydration is a key determinant of the folding, dynamics, and function of proteins. In this study, temperature-dependent Fourier transform infrared (FTIR) spectroscopy combined with singular value decomposition (SVD) and global fitting were used to investigate both the interaction of water with *α*-helical proteins and the cooperative thermal unfolding of these proteins. This methodology has been applied to an isolated *α*-helix (Fs peptide) and to globular α-helical proteins including the helical subdomain and full-length villin headpiece (HP36 and HP67). The results suggest a unique IR signature for the interaction of water with the helical amide carbonyl groups of the peptide backbone. The IR spectra indicate a weakening of the net hydrogen bond strength of water to the backbone carbonyls with increasing temperature. This weakening of the backbone solvation occurs as a discrete transition near the maximum of the temperature-dependent hydrophobic effect, not a continuous change with increasing temperature. Possible molecular origins of this effect are discussed with respect to previous molecular dynamics simulations of the temperature-dependent solvation of the helix backbone.

Protein folding, stability, and function depend on the properties of water in complex ways that are not completely understood. The influence of solvent arises from the interplay between the water and protein structures and their dynamics, including entropic effects, disruption of water structure, solvation of hydrophobic groups, and hydrogen bonding interactions.[1,2] The hydrophobic effect is thought to be a key driving force of protein folding, because it favors the folded structure in which hydrophobic residues are sequestered

[*]**Corresponding Author**: briandyer@emory.edu; phone: (404) 727-6637. .

The authors declare no competing financial interest.

from solvent within the hydrophobic core of the protein. Consequently, understanding the interactions between aqueous solvent and proteins, including hydrophobic hydration, has been the subject of numerous experimental and theoretical studies.[3-16] Several general principles have emerged from this work. The free energy change associated with the hydration of hydrophobic molecules is governed primarily by the associated changes in water structure.[17] The temperature dependence of the hydrophobic effect parallels the temperature-dependent solubility of hydrophobic or nonpolar molecules. The solubility of hydrophobic molecules in water initially decreases with increasing temperature, followed by an increase in solubility with increasing temperature, resulting in a minimum in solubility, usually above room temperature.[1] More insight into the nature of the interaction of water with proteins has come from theoretical studies, including density functional theory (DFT) calculations[3-6] and molecular dynamics (MD) simulations.[7-9,11,18] Such studies provide a wealth of molecular detail about the interaction of water with proteins, but the conclusions have been difficult to validate experimentally.

Infrared spectroscopy is an established method for the study of protein conformation,[3,4,12-16,19-22] but it also has the potential to elucidate protein–solvent interactions. The amide I band in particular is sensitive to hydrogen bonding within the protein and between the protein and the aqueous solvent.[12-16,23-25] An important example is the distinct vibrational frequencies observed for “solvated” versus “buried” helices: amide carbonyl groups involved in H-bonding within the helix and with the solvent occur at a lower frequency (~1632 cm^{-1}) than helical amide carbonyl groups that are sequestered from solvent (~1652 cm^{-1}) in the hydrophobic core of proteins or within a lipid bilayer.[14,26,27] The direct effect of hydrogen-bonding on the amide I band is that it reduces the force constant of the individual amide oscillators relative to the non-hydrogen-bonded case. The solvent also indirectly affects the amide I band by changing conformational preferences, which in turn, results in different coupling strengths. Several theoretical studies have attempted to quantify these effects.[3,4,6,28,29] An MD simulation of a solvated helical peptide found the calculated amide I band to be near 1630 cm^{-1} at low temperature, shifted by ~12 cm^{-1} toward the lower frequency compared with the buried one at room temperature.[30] The simulation suggests that the major contribution to the observed frequency shift of the amide I band arises from the strong tendency for carbonyls to form additional hydrogen bonds with water even though they are internally hydrogen bonded. In the present study, we use temperature-dependent FTIR spectroscopy combined with singular value decomposition (SVD)[31,32] and global fitting to probe the temperature-dependent hydration of unlabeled helical peptides and proteins in aqueous solutions. Although the IR spectral signature for solvated helical carbonyl groups is well-known, the difficulty in probing protein hydration arises in part from separating temperature-dependent protein solvation from the global thermal melt or unfolding of the peptide or protein. Our approach utilizes SVD and global fitting to separate these two processes, allowing the temperature dependence of the hydration of peptides and proteins to be investigated. Specifically, we studied the temperature dependence of a monomeric α-helix, the F_S peptide.[26] This peptide serves as a model for the study of two helical proteins, the villin headpiece subdomain (HP36)[12,33-37] and the villin headpiece (HP67).[38,39] The data indicate a decrease in solvent interaction with the peptide backbone as the temperature is increased over the temperature range from low temperature to the start of the unfolding transition. This weakening of the backbone solvation occurs as a discrete transition, not a continuous change with increasing temperature. Furthermore, it occurs near the maximum of the temperature-dependent hydrophobic effect. Possible molecular origins of this effect are discussed with respect to previous MD simulations of the temperature-dependent solvation of the polypeptide backbone.

MATERIALS AND METHODS

Sample Preparation

The 21-residue helical F_s peptide (succinyl-AAAAA-$(AAARA)_3$A-NH_2) was synthesized by standard Fmoc peptide synthesis. A coil reference peptide with the sequence GKAVAAK was synthesized in the same manner. The 36-residue three-helix bundle villin headpiece subdomain (HP36) was also synthesized using standard Fmoc protocols. HP36 is the C-terminal subdomain of the villin headpiece domain: MLSDEDFKAVFGMTRSAFANLPLWKQQNLKKEKGLF. The C-terminus is amidated for synthetic convenience. We use the numbering system corresponding to the full-length villin headpiece (the first leucine is designated Leu-42). The first residue Met41 is included because prior studies of recombinant versions of the headpiece helical subdomain included an additional N-terminal Met, although this residue is not found in the native intact headpiece. The 67-residue helical villin headpiece (HP67) was prepared recombinantly and has the following sequence: PTKLETFPLDVLV NTAAEDLPRGVDPSRKENHLSDEDFKAVFGMTRSAFANLPLWKQQNLKKEKGLF. The samples were purified via reverse phase HPLC and lyophilized from D_2O (Cambridge Isotopes) to exchange the amide protons with deuterium. The peptide and protein samples were dissolved in D_2O at a pH* of 4.1 (F_s peptide) or in a buffer containing 10 mM sodium phosphate and 150 mM sodium chloride at a pH* of 5.3 in D_2O (HP36) or 10 mM sodium phosphate at a pH* of 6.9 in D_2O (HP67). pH* refers to the uncorrected (for D_2O) pH-meter reading at 25 °C. The protein solutions were filtered to remove any aggregates present and used without any further purification. Samples used for the IR experiments had concentrations of ~0.2–2 mM.

Temperature-Dependent FTIR Measurements

Temperature-dependent FTIR spectra were recorded on a Bio-Rad FTS 60A FTIR spectrometer equipped with a liquid-nitrogen cooled mercury cadmium telluride (MCT) detector. Typical spectra were signal averaged for 128–512 scans at a resolution of 2 cm^{-1}. A split IR cell composed of CaF_2 windows was utilized with a path length of ~100 μm to record the spectrum of both the reference (buffer in D_2O) and the sample (protein in the D_2O buffer) side of the IR transmission cell under identical conditions at each temperature. The temperature of the IR cell was controlled by a water bath, and the sample temperature was measured by a thermocouple attached to the cell. The absorbance spectra of the protein were determined from the negative logarithm of the ratio of the single beam spectra of the sample to the reference side of the IR split cell at each temperature. The thermal unfolding of the peptide/proteins was found to be reversible by comparing the spectrum at the starting temperature to the spectrum after thermal cycling.

Singular Value Decomposition and Global Fitting

Singular value decomposition (SVD)[31] was utilized to determine the number of spectral components required to describe the temperature dependence of the protein difference FTIR spectra. These temperature-dependent difference FTIR spectra were used to construct the data matrix, $A(\tilde{\nu}, T)$, where each column represents the difference FTIR spectrum at a specific temperature. The SVD analysis of this data matrix results in three matrices, $A = USV^T$ where the U, S, and V^T matrices contain the basis spectra, the singular values and the temperature-evolution of the basis spectra, respectively. These matrices were truncated retaining the components containing signal, while removing components containing only noise. Multiple basis spectra were found to describe the original data matrix for each protein. A global fitting protocol was employed to determine the individual spectral components and the temperature dependence of these basis spectra. The $A(\tilde{\nu}, T)$ matrix is equal to both USV^T and DF^T, where the D and F^T matrices contain the individual spectral

components and their temperature dependence, respectively. Consequently, the D matrix is equal to USV^TF^{T+} where F^{T+} is the pseudoinverse of F^T. This equation can be rewritten as $D = USH$, where $H = V^TF^{T+}$. The H matrix can be determined from globally fitting the V^T matrix with the appropriate mathematical model consisting of one function for each component. The model used here consists of two sigmoid functions to determine the H matrix as shown in eq 1:

$$\begin{aligned} f(T)_1 &= h_{11} * \left(b_1 + \frac{m_1}{1+\exp\left(\left(T_{m_1} - T\right)/\delta_1\right)} \right) + h_{12} * \left(b_2 + \frac{m_2}{1+\exp\left(\left(T_{m_2} - T\right)/\delta_2\right)} \right) \\ f(T)_2 &= h_{21} * \left(b_1 + \frac{m_1}{1+\exp\left(\left(T_{m_1} - T\right)/\delta_1\right)} \right) + h_{22} * \left(b_2 + \frac{m_2}{1+\exp\left(\left(T_{m_2} - T\right)/\delta_2\right)} \right) \end{aligned} \quad (1)$$

where h_{11}, h_{12}, h_{21}, and h_{22} are the elements of the H matrix and T_m and δ represent the midpoint and width of the thermal transition, respectively (one for each sigmoid function). Two sigmoid functions were used because this represents the simplest model to globally fit the spectral components found for the temperature dependence of the proteins studied. On the basis of this global fitting protocol, the F^T matrix can be determined from the equation, $F^T = H^{-1}V^T$. The SVD analysis and global fitting were performed in IGOR Pro (WaveMetrics, Inc.).

RESULTS AND DISCUSSION

F_s Peptide

Figure 1A shows the temperature-dependent difference FTIR spectra for the F_s peptide in the amide I' region from all of the carbonyl stretching vibrations of the backbone amide groups. The difference spectra show a region (~1604 cm^{-1} to 1640 cm^{-1}) of decreasing intensity with increasing temperature indicative of both the thermal melt of the peptide in addition to changes in peptide hydration. The region (~1640 cm^{-1} to 1708 cm^{-1}) of increasing intensity with increasing temperature is due to the formation of disordered regions of the peptide, while the negative feature at ~1668 cm^{-1} is due to a TFA impurity in the sample (from the HPLC purification of the peptide). The difference spectra do not contain an isosbestic point, which usually means that more than two states and more than a single transition are present over this temperature range.

The multiple transitions present in the difference FTIR spectra of Figure 1A were resolved by a combined SVD and global fitting protocol. Figure 1B shows the first two D-matrix spectral components and the inset shows the corresponding temperature dependence of these spectral components. The two D-matrix spectral components are effectively the temperature-dependent difference spectra of the two transitions. The first (largest amplitude) D-matrix spectral component has a negative band at 1633 cm^{-1} due to the loss of helical structure with a simultaneous increase of disordered structure at 1659 cm^{-1} and 1680 cm^{-1} (this feature is a single broad band with a dip in the middle due to the TFA impurity). Thus, the first D-matrix spectral component represents a transition that involves the conversion of helical to disordered structure with an apparent T_m of ~54 °C (defined as the temperature at which half the total signal change has occurred) as determined from the corresponding F^T thermal profile. This spectral component represents the dominant process in the melt since it is the largest amplitude component. The transition is broad as expected because of the low cooperativity and extensive end-fraying characteristic of the melting transition of isolated helices.

The second D-matrix spectral component shown in Figure 1B is composed of difference features at 1621 and 1649 cm^{-1}. Because these difference features are more closely spaced, the minima and maxima do not correspond directly to the absorbance maxima (they are

lower and higher, respectively). These features are within the characteristic range of the solvated and buried helix bands. On the basis of the temperature-profile of this spectral component, the solvated helical signature decreases while the buried or partially desolvated component increases as the temperature is increased prior to the thermal melt of the peptide. This second spectral component has an apparent T_m of 28 °C determined from the corresponding F^T thermal profile. On the basis of these specific spectral features, we assign the first D-matrix spectral component to the helix-coil transition and the second component to the temperature-dependence of the hydration of the peptide backbone, prior to the thermal melt. The observation of the second component is clear evidence for a discrete, cooperative pretransition as the temperature is raised from the lowest temperature probed (11 °C) up to the global melt of the helical peptide. This pretransition is characterized by a weakening of the effective hydrogen bonding strength to the helical carbonyl groups, consistent with a loss of solvent interaction with the backbone, or at least a weakening of that interaction. It is analogous to the temperature-dependent changes previously observed for the solvated helix band of GCN-4 and α_3D using isotope labeling.[13,15] By extending the temperature range of our measurements to higher temperature than the previous work, and using the SVD approach, we are able to observe the weakening of solvent hydrogen bonding to the peptide as a discrete transition, rather than a continuous change with temperature.

Reference Coil Peptide

A control experiment was performed using a reference coil peptide with the sequence GKAVAAK that is disordered over the temperature range from 5 to 50 °C. The control peptide allows us to follow any changes in backbone solvation in the absence of a global conformational change. The temperature-dependent difference FTIR spectra of this reference peptide is shown in Figure 2A. The difference spectra exhibit broad negative (1640 cm^{-1}) and positive (above 1660 cm^{-1}) components. These components correspond to solvent protected and fully solvated disordered structure, respectively. A sharp negative feature at 1670 cm^{-1} is due to a TFA impurity in this sample. The data are well modeled by a single broad sigmoidal transition with a T_m of 34 °C as shown in Figure 2B. Thus, even in the absence of any global conformational change, we observe a change in the solvation of the peptide backbone as the temperature is raised. We emphasize that this change is not continuous with temperature but instead exhibits a specific transition with a T_m close to that observed for the helical F_s peptide system.

Villin Headpiece Subdomain (HP36)

The villin headpiece subdomain (HP36) is a 36-residue, three-helix bundle protein. The protein is composed of two short N-terminal helices (Asp44–Lys48 and Arg55–Phe58) and a longer C-terminal helix (Leu63–Glu72). Figure 3A shows the temperature-dependent difference FTIR spectra of this 36-residue helical protein from 3 to 93 °C in ~5 °C increments. The difference spectra exhibit negative (1610 cm^{-1} to 1655 cm^{-1}) and positive (1655 cm^{-1} to 1730 cm^{-1}) regions that grow in intensity with increasing temperature, indicating the loss of secondary and tertiary structure with a simultaneous increase in disordered regions of the protein, respectively. Two helical bands appear at 1630 cm^{-1} and 1645 cm^{-1} due to solvated and buried helical components. These components show different melt profiles as shown in Figure 3A (inset). The 1630 cm^{-1} component shows a broader melt profile with a sloping pretransition baseline, whereas the 1645 cm^{-1} melt curve shows a more cooperative melt without a sloping pretransition baseline and reflects the disruption of the hydrophobic core. The observation of frequency-dependent melt profiles and the lack of an isosbestic point in the difference spectra suggest the presence of more than one temperature-dependent process.

We emphasize that these single frequency melt curves are less accurate than the curves obtained from the SVD analysis, because the latter are obtained using the full frequency dependence of the absorbance spectra. A combined SVD and global fitting protocol applied to the temperature dependence of HP36 showed two statistically significant spectral components. The two D-matrix spectral components are shown in Figure 3B with the corresponding temperature dependences (F^T-matrix) shown in the inset. Similar to the F_S peptide, the first D-matrix spectral component resembles the higher temperature difference FTIR spectra. The component has two prominent characteristic helical bands. The predominant band at 1644 cm^{-1} is due to desolvated or buried amide carbonyl groups, while the less intense 1631 cm^{-1} band is due to solvated amide carbonyl groups. The corresponding temperature dependence follows the disruption of the hydrophobic core signifying the global melt of the protein and an increase in solvated helical amide carbonyl groups.

The second D-matrix spectral component shows difference features at 1626 and 1658 cm^{-1}. As was the case for F_S peptide, these difference features are close enough that they likely do not correspond to the actual absorbance maxima (they are lower and higher, respectively), and they span the range expected for solvated and buried helix. The temperature dependence of these bands suggests the loss of solvated carbonyl groups with a concurrent increase of desolvated groups as the temperature is increased from lowest temperature probed (3 °C) until the global unfolding of this three-helix bundle protein. The apparent T_m for this transition is 18 °C, which is similar to the temperature dependence of the second component for F_S peptide. These results suggest an apparent desolvation or weakening of water hydrogen bonds to the helical amide carbonyl groups as the temperature is raised prior to the global melt (crossing the primary activation barrier to unfolding). The solvation of the protein starts to increase once global unfolding starts. The pretransition observed prior to the global unfolding is likely due to disruption of H-bonds between the solvent and helical amide carbonyl groups on the surface of the protein.

Villin Headpiece (HP67)

The villin headpiece (HP67) is the full-length, 67-residue protein from which HP36 is derived. The C-terminal subdomain of this construct is HP36, while the N-terminal subdomain is composed primarily of loop and turn regions along with a four-residue α-helix and three residues with ϕ and ψ dihedral angles consistent with a 3_{10}-helix. This larger protein is more stable, has a slightly larger hydrophobic core and yet little additional helix, and thus serves as an interesting comparison to the more solvent exposed helices of FTIR spectra of this 67-residue helical protein from 5 to 87 °C in ~5 °C increments. Like HP36, the difference FTIR spectra have regions of negative (1611 cm^{-1} to 1657 cm^{-1}) and positive (1657 cm^{-1} to 1730 cm^{-1}) intensity that increase in intensity with increasing temperature. The negative bands are primarily due to the loss of secondary and tertiary structure, while the positive bands are primarily due to the formation of disordered regions of the protein.

Unlike HP36, HP67 exhibits a single negative band at 1637 cm^{-1} instead of two distinct bands for solvated and buried helical carbonyl groups. This difference is due to the melt of turn regions in the N-terminal subdomain of HP67, which overlap with bands due to solvated and buried helical amide carbonyl groups. The temperature-dependent difference FTIR spectra of HP67 do not show an isosbestic point. This is consistent with earlier NMR studies that showed the folding of this protein is not two-state.[38,39] The minimum model needed to describe the unfolding includes two intermediates, one with a folded C-terminal subdomain and a partially unfolded N-terminal subdomain and the second with a folded C-terminal subdomain but unfolded N-terminal subdomain.

A combined SVD and global fitting analysis of the temperature-dependent difference FTIR spectra in Figure 4A yields two spectral components. The first and second D-matrix spectral components show similarities to the high and low temperature difference FTIR spectra, respectively. The F^T-temperature profiles for the first and second D-spectral components exhibit apparent T_m's of ~69 °C and ~24 °C, respectively (inset). The first D-matrix spectral component shows a negative band at 1642 cm^{-1} due to the loss of tertiary structure and a positive band at 1680 cm^{-1} due to the formation of disordered regions of the protein upon the global thermally induced unfolding of HP67 as confirmed by the corresponding F^T-temperature profile. The second D-spectral component contains one dominant positive band at 1633 cm^{-1} due to solvated helix. The corresponding F^T-temperature profile shows that the amount of solvated carbonyl groups decreases as the temperature is raised from the lowest temperature probed (5 °C) until the global melt of the protein. This result is in agreement with the F_S peptide and HP36 cases, consistent with a weakening of hydrogen bonding to solvent of helical amide carbonyl groups that occurs prior to the global melt of the helical protein.

Comparison to Simulations

All of the proteins examined in the present study exhibit a pretransition in the temperature-dependent FTIR spectra that we interpret as a weakening of the hydrogen bonding between solvent and the peptide backbone. This change in solvation is even observed for the unstructured control peptide, and in all cases is manifested as a transition that occurs independently of any global structural transition (e.g., unfolding). Some insight into the molecular origin of the temperature-dependent solvation effects is provided by previous REMD simulations of a helical peptide (AK) that considered how temperature effects are manifested in the amide I spectrum.[30,40] The AK peptide is a reasonable model system for comparison because it forms a stable helix in aqueous solution, is well characterized experimentally, and is closely related structurally to the F_S peptide.[41-44] The simulations provide a solid structural basis for interpreting observations from linear IR by taking into account peptide carbonyl (C=O) hydrogen-bonding to backbone NH groups (internal) and water (external) and the coupling between amide I modes as a function of temperature.

The MD simulations capture an initial desolvation of the helix (measured as a loss of frequency shift due backbone C=O hydrogen-bonding to solvent) at lower temperature, prior to the major unfolding transition.[30,40] Interestingly, certain positions within the helix contribute more to the frequency shift than others at lower temperature, depending on the degree of shielding of the backbone by the Lys side chains. The observed pretransition desolvation is most prominent at exposed or solvated positions and minimal at shielded or buried positions. The nature of the observed backbone desolvation is a decrease in the number of hydrogen bonds between the backbone carbonyls and water. Deviations in internal helical hydrogen bonding or in the solvent-hydrogen bond structure were not observed. The FTIR data analysis is consistent with the picture that emerges from the MD simulations. The pretransition exhibits no change in the buried helix band, indicating that the global structure of the protein remains intact, whereas the solvated helix band is shifted toward higher frequency, consistent with a reduction in the effective hydrogen bond strength with water. We postulate that this weakening of the backbone solvation is due to a change in the number of hydrogen bonds to water, on the basis of the simulations.

CONCLUSIONS

The results presented here demonstrate the ability of temperature-dependent FTIR spectroscopy in conjunction with a combined SVD and global fitting analysis to elucidate both the thermal unfolding of proteins and the temperature-dependent solvation of the peptide backbone. The results suggest a decrease in the hydration or hydrogen bond strength

between water and the amide carbonyls with increasing temperature in the low temperature range below the unfolding transition. We have observed this temperature-dependent interaction of water with helical carbonyl groups for a range of α-helical structures and thus it appears to be a general phenomenon. The pretransition is characterized by similar spectral features and a similar apparent T_m (18, 24, and 28 °C) regardless of the specific protein sequence.

There are several possible origins of this temperature-dependent change in backbone solvation, including water structural rearrangement in response to local protein structural changes; changes in the water structure induced in the absence of any protein structural changes; or amino acid side chain shielding of the peptide backbone. REMD simulations of the AK helical peptide are most consistent with the last two possibilities. The simulations show that the temperature-dependent desolvation is primarily a consequence of the change in the number of hydrogen bonds between the amide carbonyls and water molecules. The simulations also show modulation of the backbone solvation by side chain interactions. Similarly, MD simulations of the Fs peptide have suggested that the Arg side chains shield the backbone amide carbonyl groups in this case.[7] This type of shielding is likely responsible, at least in part, for the temperature-dependent solvation of surface helical amide carbonyl groups.

The observed temperature dependence of the backbone solvation appears to be correlated to the temperature dependence of the hydrophobic effect.[1,8,10,45] The solubility of hydrophobic side chains is higher at low and high temperature with a minimum at intermediate temperatures, usually between 310 and 330 K. Therefore, hydrophobic amino acid side chains on the surface of the protein could be more hydrated at low temperatures due to a lower free energy barrier to hydration. As the temperature is raised, the hydrophobic effect is expected to increase, potentially leading to the shielding of peptide backbone amide carbonyl groups as the side chains interacts more with the backbone to decrease side chain hydration. In this scenario, there is a delicate balance between enthalpic and entropic factors affecting protein stability, structure and solvent interaction.

Further study would be required to determine the generality of the temperature dependence of protein–solvent interactions, especially for β-sheets containing peptides and proteins. The temperature dependence of the hydrophobic effect suggests that the observed protein hydration trends are indeed general. Temperature-dependent protein hydration will play a role in the interpretation of the protein folding dynamics. For instance, temperature-induced relaxation methods probing the folding and unfolding kinetics of several helical proteins have shown biphasic relaxation kinetics.[12,14,33,46] The slower phase is related to the global folding/unfolding of the protein involving the formation/disruption of the hydrophobic core, while the faster kinetic phase (~10^7 s^{-1}) has been assigned to the helix-coil of these processes have to be viewed in terms of temperature-dependent protein hydration prior to, during, and after the global folding/unfolding of the protein.

Acknowledgments

Funding

This work was funded by NIH Grant GM 053640 to R.B.D. and NSF Grant MCB-0919860 to D.P.R.

ABBREVIATIONS

FTIR Fourier transform infrared

SVD	singular value decomposition
REMD	replica exchange molecular dynamics
TFA	trifluoroacetic acid
HP36	villin headpiece subdomain
HP67	villin headpiece

REFERENCES

(1). Widom B, Bhimalapuram P, Koga K. The hydrophobic effect. Phys. Chem. Chem. Phys. 2003; 5:3085–3093.

(2). Sharp KA, Vanderkooi JM. Water in the half shell: structure of water, focusing on angular structure and solvation. Acc. Chem. Res. 2010; 43:231–239. [PubMed: 19845327]

(3). Kubelka J, Huang R, Keiderling TA. Solvent effects on IR and VCD spectra of helical peptides: DFT-based static spectral simulations with explicit water. J. Phys. Chem. B. 2005; 109:8231–8243. [PubMed: 16851962]

(4). Turner DR, Kubelka J. Infrared and vibrational CD spectra of partially solvated {alpha}-helices: DFT-based simulations with explicit solvent. J. Phys. Chem. B. 2007; 111:1834–1845. [PubMed: 17256894]

(5). Kubelka J, Keiderling TA. Ab initio calculation of amide carbonyl stretch vibrational frequencies in solution with modified basis sets. 1: N-methyl acetamide. J. Phys. Chem. A. 2001; 105:10922–10928.

(6). Bour P, Kubelka J, Keiderling TA. Ab initio quantum mechanical models of peptide helices and their vibrational spectra. Biopolymers. 2002; 65:45–59. [PubMed: 12209472]

(7). Garcia AE, Sanbonmatsu KY. alpha-Helical stabilization by side chain shielding of backbone hydrogen bonds. Proc. Natl. Acad. Sci. U. S. A. 2002; 99:2782–2787. [PubMed: 11867710]

(8). Hummer G, Garde S, Garcia AE, Pratt LR. New perspectives on hydrophobic effects. Chem. Phys. 2000; 258:349–370.

(9). Garcia AE, Hummer G, Soumpasis DM. Hydration of an alpha-helical peptide: Comparison of theory and molecular dynamics simulation. Proteins: Struct., Funct., Genet. 1997; 27:471–480. [PubMed: 9141128]

(10). Hummer G, Garde S, Garcia AE, Paulaitis ME, Pratt LR. Hydrophobic effects on a molecular scale. J. Phys. Chem. B. 1998; 102:10469–10482.

(11). Huang DM, Chandler D. The hydrophobic effect and the influence of solute-solvent attractions. J. Phys. Chem. B. 2002; 106:2047–2053.

(12). Brewer SH, Vu DM, Tang YF, Li Y, Franzen S, Raleigh DP, Dyer RB. Effect of modulating unfolded state structure on the folding kinetics of the villin headpiece subdomain. Proc. Natl. Acad. Sci. U. S. A. 2005; 102:16662–16667. [PubMed: 16269546]

(13). Manas ES, Getahun Z, Wright WW, DeGrado WF, Vanderkooi JM. Infrared spectra of amide groups in alpha- helical proteins: Evidence for hydrogen bonding between helices and water. J. Am. Chem. Soc. 2000; 122:9883–9890.

(14). Vu DM, Myers JK, Oas TG, Dyer RB. Probing the folding and unfolding dynamics of secondary and tertiary structres in a three-helix bundle protein. Biochemistry. 2004; 43:3582–3589. [PubMed: 15035628]

(15). Walsh STR, Cheng RP, Wright WW, Alonso DOV, Daggett V, Vanderkooi JM, DeGrado WF. The hydration of amides in helices; a comprehensive picture from molecular dynamics, IR, and NMR. Protein Sci. 2003; 12:520–531. [PubMed: 12592022]

(16). Zhu Y, Alonso DOV, Maki K, Huang CY, Lahr SJ, Daggett V, Roder H, DeGrado WF, Gai F. Ultrafast folding of alpha(3): A de novo designed three-helix bundle protein. Proc. Natl. Acad. Sci. U. S. A. 2003; 100:15486–15491. [PubMed: 14671331]

(17). Scheraga HA. Theory of hydrophobic interactions. J. Biomol. Struct. Dyn. 1998; 16:447–460. [PubMed: 9833681]

(18). Ghosh T, Garde S, Garcia AE. Role of backbone hydration and salt-bridge formation in stability of alpha-helix in solution. Biophys. J. 2003; 85:3187–3193. [PubMed: 14581218]

(19). Fang C, Wang J, Kim YS, Charnley AK, Barber- Armstrong W, Smith AB III, Decatur SM, Hochstrasser RM. Two-dimensional infrared spectroscopy of isotopomers of an alanine rich alpha-helix. J. Phys. Chem. B. 2004; 108:10415–10427.

(20). Huang R, Kubelka J, Barber-Armstrong W, Silva RAGD, Decatur SM, Keiderling TA. Nature of vibrational coupling in helical peptides: An isotopic labeling study. J. Am. Chem. Soc. 2004; 126:2346–2354. [PubMed: 14982438]

(21). Lednev IK, Karnoup AS, Sparrow MC, Asher SA. Transient UV Raman spectroscopy finds no crossing barrier between the peptide alpha-helix and fully random coil conformation. J. Am. Chem. Soc. 2001; 123:2388–2392. [PubMed: 11456888]

(22). Mukherjee S, Chowdhury P, Gai F. Infrared study of the effect of hydration on the amide I band and aggregation properties of helical peptides. J Phys Chem B. 2007; 111:4596–4602. [PubMed: 17419612]

(23). Werner JH, Dyer RB, Fesinmeyer RM, Andersen NH. Dynamics of the primary processes of protein folding: helix nucleation. J. Phys. Chem. B. 2002; 106:487–494.

(24). Torii H, Tasumi M. Model-calculations on the amide-I infrared bands of globular-proteins. J. Chem. Phys. 1992; 96:3379–3387.

(25). Kimura T, Maeda A, Nishiguchi S, Ishimori K, Morishima I, Konno T, Goto Y, Takahashi S. Dehydration of main- chain amides in the final folding step of single-chain monellin revealed by time-resolved infrared spectroscopy. Proc. Natl. Acad. Sci. U. S. A. 2008; 105:13391–13396. [PubMed: 18757727]

(26). Williams S, Causgrove TP, Gilmanshin R, Fang KS, Callender RH, Woodruff WH, Dyer RB. Fast events in protein folding: Helix melting and formation in a small peptide. Biochemistry. 1996; 35:691–697. [PubMed: 8547249]

(27). Starzyk A, Barber-Armstrong W, Sridharan M, Decatur SM. Spectroscopic evidence for backbone desolvation of helical peptides by 2,2,2-trifluoroethanol: An isotope-edited FTIR study. Biochemistry. 2005; 44:369–376. [PubMed: 15628879]

(28). Lin YS, Shorb JM, Mukherjee P, Zanni MT, Skinner JL. Empirical amide I vibrational frequency map: Application to 2D-IR line shapes for isotope-edited membrane peptide bundles. J. Phys. Chem. B. 2009; 113:592–602. [PubMed: 19053670]

(29). Wang L, Middleton CT, Zanni MT, Skinner JL. Development and validation of transferable amide I vibrational frequency maps for peptides. J. Phys. Chem. B. 2011; 115:3713–3724. [PubMed: 21405034]

(30). Gnanakaran S, Hochstrasser RM, Garcia AE. Nature of structural inhomogeneities on folding a helix and their influence on spectral measurements. Proc. Natl. Acad. Sci. U.S.A. 2004; 101:9229–9234. [PubMed: 15197256]

(31). Hendler RW, Shrager RI. Deconvolutions based on singular value decomposition and the pseudoinverse: A guide for beginners. J. Biochem. Biophys. Methods. 1994; 28:1–33. [PubMed: 8151067]

(32). Henry, ER.; Hofrichter, J.; Brand, L.; Johnson, ML. Methods in Enzymology. Academic Press Ltd.; London, England, UK: 1992. Singular value decomposition: Application to analysis of experimental data; p. 129-192.

(33). Brewer SH, Song BB, Raleigh DP, Dyer RB. Residue specific resolution of protein folding dynamics using isotope- edited infrared temperature jump spectroscopy. Biochemistry. 2007; 46:3279–3285. [PubMed: 17305369]

(34). Wang MH, Tang YF, Sato SS, Vugmeyster L, McKnight CJ, Raleigh DP. Dynamic NMR line-shape analysis demonstrates that the villin headpiece subdomain folds on the microsecond time scale. J. Am. Chem. Soc. 2003; 125:6032–6033. [PubMed: 12785814]

(35). Bowman GR, Pande VS. Protein folded states are kinetic hubs. Proc. Natl. Acad. Sci. U. S. A. 2010; 107:10890–10895. [PubMed: 20534497]

(36). Ensign DL, Kasson PM, Pande VS. Heterogeneity even at the speed limit of folding: Large-scale molecular dynamics study of a fast-folding variant of the villin headpiece. J. Mol. Biol. 2007; 374:806–816. [PubMed: 17950314]

(37). Lei HX, Chen CJ, Xiao Y, Duan Y. The protein folding network indicates that the ultrafast folding mutant of villin headpiece subdomain has a deeper folding funnel. J. Chem. Phys. 2011; 134

(38). Tang YF, Grey MJ, McKnight J, Palmer AG, Raleigh DP. Multistate folding of the villin headpiece domain. J. Mol. Biol. 2006; 355:1066–1077. [PubMed: 16337228]

(39). Grey MJ, Tang YF, Alexov E, McKnight CJ, Raleigh DP, Palmer AG. Characterizing a partially folded intermediate of the villin headpiece domain under non-denaturing conditions: Contribution of His41 to the pH-dependent stability of the N-terminal subdomain. J. Mol. Biol. 2006; 355:1078–1094. [PubMed: 16332376]

(40). Paschek D, Gnanakaran S, Garcia AE. Simulations of the pressure and temperature unfoldiong of an a- helical peptide. Proc. Natl. Acad. Sci. U.S.A. 2005; 102:6765–6770. [PubMed: 15800045]

(41). Decatur SM, Antonic J. Isotope-edited infrared spectroscopy of helical peptides. J. Am. Chem. Soc. 1999; 121:11914–11915.

(42). Zanni MT, Hochstrasser RM. Two-dimensional infrared spectroscopy: a promising new method for the time resolution of structures. Curr. Opin. Struct. Biol. 2001; 11:516–522. [PubMed: 11785750]

(43). Silva RAGD, Kubelka J, Bour P, Decatur SM, Keiderling TA. Site-specific conformational determination in thermal unfolding studies of helical peptides using vibrational circular dichroism with isotopic substitution. Proc. Natl. Acad. Sci. U. S. A. 2000; 97:8318–8323. [PubMed: 10880566]

(44). Decatur SM. IR spectroscopy of isotope-labeled helical peptides: Probing the effect of N-acetylation on helix stability. Biopolymers. 2000; 54:180–185. [PubMed: 10861379]

(45). Hummer G, Garde S, Garcia AE, Pohorille A, Pratt LR. An information theory model of hydrophobic interactions. Proc. Natl. Acad. Sci. U. S. A. 1996; 93:8951–8955. [PubMed: 11607700]

(46). Kubelka J, Eaton WA, Hofrichter J. Experimental tests of villin subdomain folding simulations. J. Mol. Biol. 2003; 329:625–630. [PubMed: 12787664]

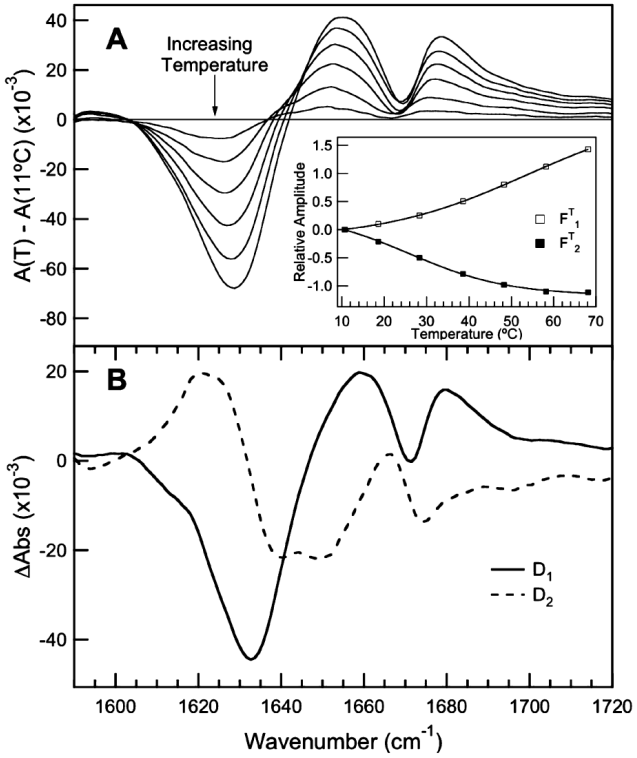

Figure 1.

Temperature-dependent FTIR difference spectra of the Fs peptide (A) measured from 11 to 68 °C in ~10 °C increments and the D-spectral components (B) with the corresponding F^T-temperature profiles (shown as an inset) determined from an SVD and global fitting analysis of the temperature-dependent FTIR difference spectra. The difference spectra are produced by subtracting the lowest temperature absorbance spectrum from the higher temperature spectra.

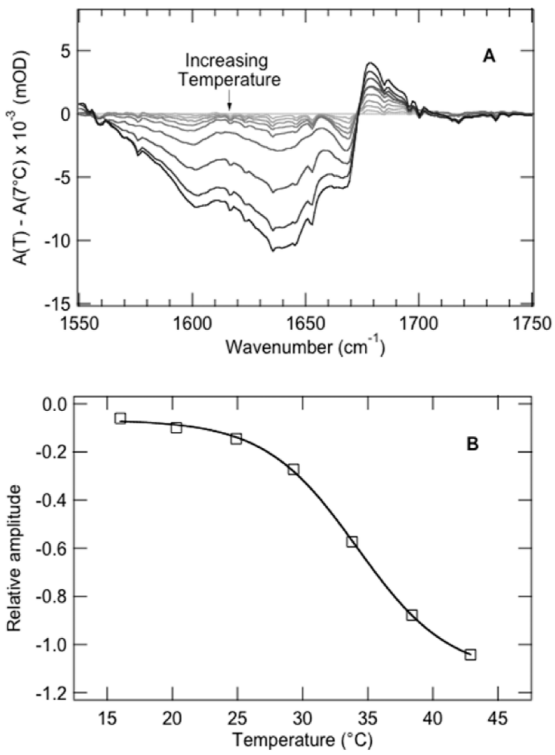

Figure 2.

(A) Temperature-dependent FTIR difference spectra of coil peptide Ac-GKAVAAK-NH_2 from 5 to 45 °C in ~5 °C increments. (B) Temperature profile obtained from the IR absorbance changes at 1645 cm^{-1}.

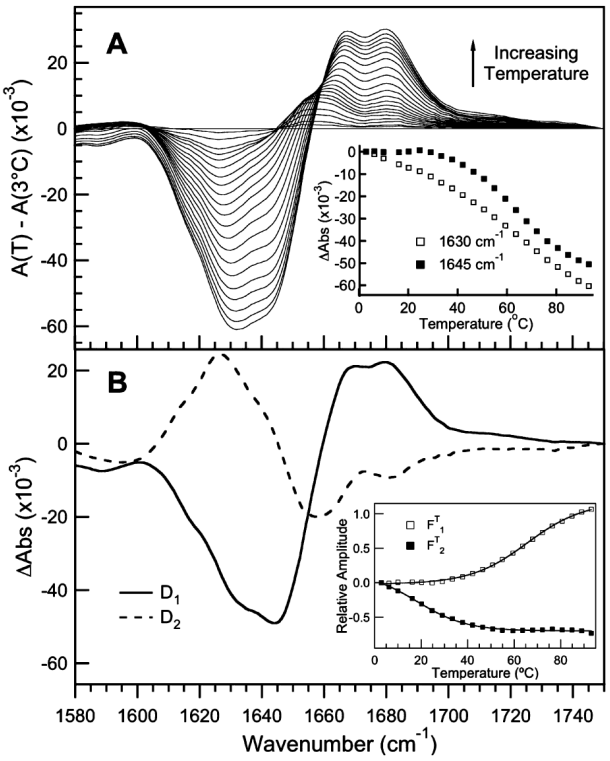

Figure 3.

Temperature-dependent FTIR difference spectra of HP36 (A) measured from 3 to 93 °C in ~5 °C increments. The temperature profiles at 1630 cm^{-1} and 1645 cm^{-1} are shown in the inset. The D-spectral components (B) and the corresponding F^T-temperature profiles (inset) determined from an SVD and global fitting analysis of the temperature-dependent FTIR difference spectra.

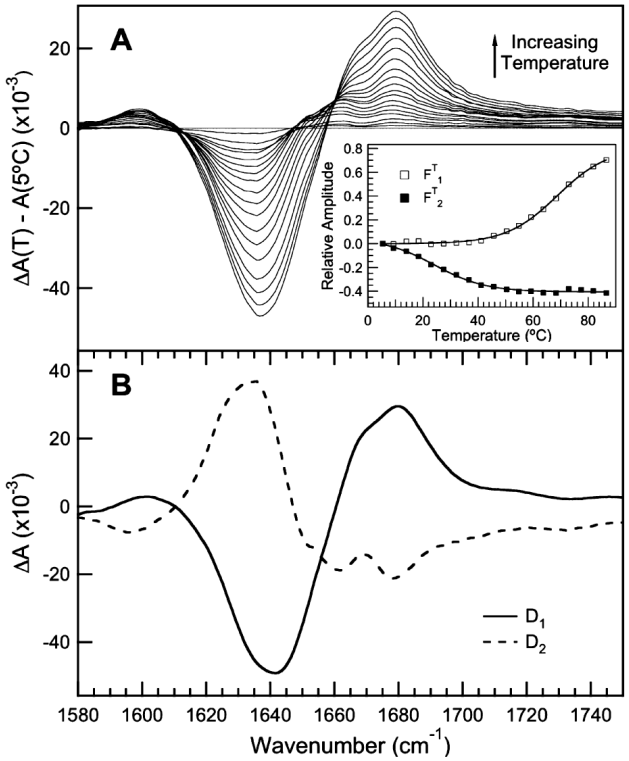

Figure 4.

Temperature-dependent FTIR difference spectra of HP67 (A) measured from 5 to 87 °C in ~5 °C increments. The D-spectral components (B) and the corresponding F^T-temperature profiles (inset) determined from an SVD and global fitting analysis of the temperature-dependent FTIR difference spectra.